Published OnlineFirst November 5, 2013; DOI: 10.1158/1535-7163.MCT-13-0225-T

Molecular Cancer Therapeutics

Phosphoproteomic Profiling Identifies Focal Adhesion Kinase as a Mediator of Docetaxel Resistance in Castrate-Resistant Prostate Cancer

Brian Y. Lee, Falko Hochgräfe, Hui-Ming Lin, et al.

Mol Cancer Ther 2014;13:190-201. Published OnlineFirst November 5, 2013.

Published OnlineFirst November 5, 2013; DOI: 10.1158/1535-7163.MCT-13-0225-T

Cancer Biology and Signal Transduction

Molecular Cancer Therapeutics

Phosphoproteomic Profiling Identifies Focal Adhesion Kinase as a Mediator of Docetaxel Resistance in Castrate-Resistant Prostate Cancer

Brian Y. Lee[1], Falko Hochgräfe[1,5], Hui-Ming Lin[1], Lesley Castillo[1], Jianmin Wu[1], Mark J. Raftery[2], S. Martin Shreeve[6], Lisa G. Horvath[1,3], and Roger J. Daly[1,4]

Abstract

Docetaxel remains the standard-of-care for men diagnosed with metastatic castrate-resistant prostate cancer (CRPC). However, only approximately 50% of patients benefit from treatment and all develop docetaxel-resistant disease. Here, we characterize global perturbations in tyrosine kinase signaling associated with docetaxel resistance and thereby develop a potential therapeutic strategy to reverse this phenotype. Using quantitative mass spectrometry–based phosphoproteomics, we identified that metastatic docetaxel-resistant prostate cancer cell lines (DU145-Rx and PC3-Rx) exhibit increased phosphorylation of focal adhesion kinase (FAK) on Y397 and Y576, in comparison with parental controls (DU145 and PC3, respectively). Bioinformatic analyses identified perturbations in pathways regulating focal adhesions and the actin cytoskeleton and in protein–protein interaction networks related to these pathways in docetaxel-resistant cells. Treatment with the FAK tyrosine kinase inhibitor (TKI) PF-00562271 reduced FAK phosphorylation in the resistant cells, but did not affect cell viability or Akt phosphorylation. Docetaxel administration reduced FAK and Akt phosphorylation, whereas cotreatment with PF-00562271 and docetaxel resulted in an additive attenuation of FAK and Akt phosphorylation and overcame the chemoresistant phenotype. The enhanced efficacy of cotreatment was due to increased autophagic cell death, rather than apoptosis. These data strongly support that enhanced FAK activation mediates chemoresistance in CRPC, and identify a potential clinical niche for FAK TKIs, where coadministration with docetaxel may be used in patients with CRPC to overcome chemoresistance. *Mol Cancer Ther; 13(1); 190–201. ©2013 AACR.*

Introduction

Prostate cancer remains the third leading cause of cancer-related death in men in the developed world (1) with castrate-resistant prostate cancer (CRPC) being the lethal stage of the disease. Docetaxel-based chemotherapy is the first-line cytotoxic treatment offering both symptomatic and survival benefits for patients diagnosed with metastatic CRPC (2, 3). However, docetaxel only clinically benefits approximately 50% of men at the cost of significant toxicity (2). Inevitably, those patients who respond develop resistance to chemotherapy. Therefore, there is an urgent need to identify novel therapeutic strategies to overcome resistance to docetaxel in patients with CRPC.

Accumulating evidence has implicated several mechanisms in the development of docetaxel resistance. These include increased drug efflux through enhanced expression of multidrug resistance proteins (MDRP; 4) and perturbations in intra- and intercellular signaling pathways. Examples of the latter mechanism include altered expression and/or activation of apoptotic regulators such as Clusterin (5), HSPs (6), IAPs (7), and Bcl2 (8) and components of growth factor signaling pathways, such as PI3-kinase/Akt/mTOR (9) and platelet-derived growth factor receptor (10). However, clinical trials emanating from these targets (11–16) have yet to make an impact in the clinical setting with the exception of cabazitaxel. Cabazitaxel is a novel tubulin-binding taxane with poor affinity for the multidrug P-glycoprotein efflux pump. A randomized phase III study (TROPIC trial) demonstrated that men with CRPC progressing after

Authors' Affiliations: [1]The Kinghorn Cancer Centre, Cancer Research Program, Garvan Institute of Medical Research, Darlinghurst; [2]Bioanalytical Mass Spectrometry Facility, University of New South Wales; [3]Royal Prince Alfred Hospital, Sydney, New South Wales; [4]Department of Biochemistry and Molecular Biology, School of Biomedical Sciences, Monash University, Melbourne, Victoria, Australia; [5]Junior Research Group Pathoproteomics, Competence Center Functional Genomics, University of Greifswald, Greifswald, Germany; and [6]Pfizer Oncology, La Jolla, California

Note: Supplementary data for this article are available at Molecular Cancer Therapeutics Online (http://mct.aacrjournals.org/).

L.G. Horvath and R.J. Daly contributed equally to this work.

Current address for S.M. Shreeve: Janssen Pharmaceutical Companies of Johnson and Johnson, 10990 Wilshire Blvd, Suite 1200, Los Angeles, CA 90024.

Corresponding Author: Roger J. Daly, Department of Biochemistry and Molecular Biology, School of Biomedical Sciences, Level 1, Building 77, Monash University, VIC 3800, Australia. Telephone: 61-3-990-29301; Fax: 61-3-990-29500; E-mail: roger.daly@monash.edu

doi: 10.1158/1535-7163.MCT-13-0225-T

Published OnlineFirst November 5, 2013; DOI: 10.1158/1535-7163.MCT-13-0225-T

docetaxel-therapy benefited from cabazitaxel treatment with an improvement in median overall survival of approximately 3 months (17). Collectively, such limited success by conventional candidate-based approaches in the clinical setting highlights an urgent need to better understand the underlying molecular mechanism of chemoresistance and design novel therapeutic strategies.

To date, no one has undertaken a global analysis of signaling networks in docetaxel-resistant CRPC. In this study, we designed an integrative approach involving characterization of aberrant phosphorylation events in docetaxel-resistant cells using quantitative mass spectrometry (MS)-based phosphoproteomic profiling, followed by functional interrogation of aberrantly activated kinases using selective tyrosine kinase inhibitors (TKI). Our findings provide important insights into the biology of chemoresistance in prostate cancer and have significant implications for the development of therapeutic strategies.

Materials and Methods

Drugs and compounds

Docetaxel (Sanofi-Aventis), PF-00562271 (Symansis), Z-VAD-FMK (R&D Systems), and 3-methyladenine (3-MA; Sigma-Aldrich) were obtained from their respective manufacturers and handled according to the manufacturer's recommendations.

Cell cultures and cell lines

PC3 and DU145 cell lines were purchased from and authenticated by the American Type Culture Collection. Docetaxel-resistant sublines (PC3-Rx and DU145-Rx) were established and maintained as previously described (18). All cell lines were used within 10 passages and for less than 3 months after reviving from frozen storage, routinely tested to confirm chemosensitivity by cell viability assay, and independently authenticated by Cell Bank Australia in May 2013 using a short tandem repeat profiling approach.

Cell viability assay

This was based on Trypan blue exclusion (18). The concentration of drug required to kill 50% of the cells (IC_{50}) was calculated, as previously described (18).

Phosphoproteomic profiling

Quantitative tyrosine phosphorylation profiling of docetaxel-sensitive and resistant cells was undertaken by immunoaffinity purification followed by liquid chromatography/tandem mass spectrometry (LC/MS-MS) in combination with stable isotope labeling with amino acids in cell culture (SILAC), as previously described (19, 20).

Pathway enrichment and protein–protein interaction network analyses

KOBAS was used to perform pathway enrichment analysis (21). The hypergeometric test was selected to test statistical enrichment of KEGG and Reactome pathways, and the *P* values were corrected for multiple comparisons (22). The protein–protein interactions among proteins of interest were retrieved from the Protein Interaction Network Analysis platform (23), and substrate–kinase relationships were downloaded from the PhosphoSitePlus database (24). Cytoscape (25) was used for visualization of networks.

Immunoblotting analysis

Preparation of cell lysates, immunoblotting, and densitometry analyses were performed as previously described (19, 26). All primary antibodies used in this study were from Cell Signaling Technology, except pY397-FAK (Invitrogen), FAK (BD Transduction Laboratories), pY576-FAK (Santa Cruz Biotechnology), β-Actin (Sigma), and GAPDH (Abcam).

Apoptosis assay

Determination of sub-G_1 phase of PC3/PC3-Rx and DU145/DU145-Rx cell lines ± docetaxel ± FAK TKI was undertaken, as previously described (19).

Colony-forming assay

Clonogenicity of the PC3/PC3-Rx and DU145/DU145-Rx models was quantified by measuring the number of surviving colonies undergoing ± docetaxel ± PF-00562271 (100 nmol/L) treatments (18).

Rhodamine assay

P-glycoprotein activity in DU145 and DU145-Rx cells was quantified by measuring Rh123 fluorescence ± P-glycoprotein inhibitor PSC833 (1 mmol/L, Novartis; ref. 18).

Small interfering RNA transfection

Atg5 small-interfering RNAs (siRNA) #7, 8 and 10 were obtained from Thermo Scientific. #7 siRNA sequence was GGCAUUAUCCAAUUGGUUU, #8 GCAGAACCAUACUAUUUGC, #10 ACAAAGAUGUGCUUCGAGA. ON-TARGET*plus* Non-Targeting Pool was obtained from Thermo Scientific. Cells were transfected with 5 to 20 nmol/L of siRNAs using Lipofectamine (Invitrogen) for 48 hours. For cell death rescue experiment with Atg5 knockdown, 5 nmol/L of siRNAs were used.

Statistical analysis

Comparisons between more than two groups were made using one-way analysis of variance (ANOVA) with Bonferroni post hoc correction for multiple comparisons. *P* values of less than 0.05 were considered statistically significant. All statistical tests were performed using GraphPad Prism 5 (GraphPad Software Inc).

Results

Phosphotyrosine profiling of docetaxel-resistant prostate cancer cells

To complement our previously established PC3/PC3-Rx model (18), we developed a second docetaxel-resistant

Published OnlineFirst November 5, 2013; DOI: 10.1158/1535-7163.MCT-13-0225-T

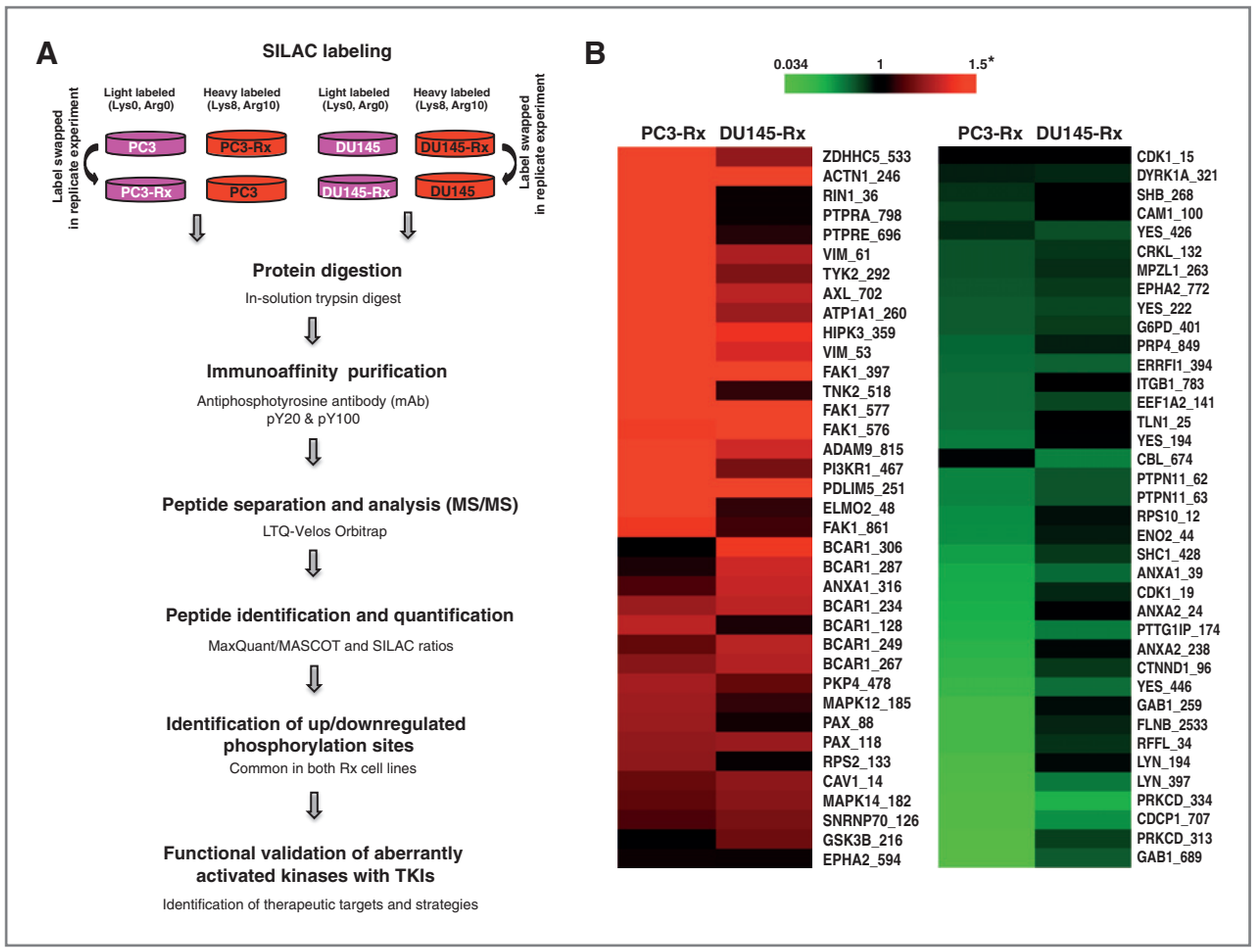

Figure 1. Phosphoproteomic profiling of docetaxel-resistant prostate cancer cells. A, workflow for quantitative phosphoproteomic profiling. B, heatmap of up- (red) or downregulated (green) tyrosine phosphorylation sites found in both PC3-Rx and DU145-Rx cell lines, in comparison with their parental cell lines (PC3 and DU145, respectively). A ranking of differentially phosphorylated sites characteristic of both docetaxel-resistant models was performed according to their SILAC ratios as indicated in the scale bar, where SILAC ratio of 1 indicates no change, and <1 indicates down-, and >1 indicates upregulated phosphosites. *, For ease of comparison, we have set the upper limit of the scale at 1.5-fold. However, many sites show larger fold changes. Absolute values are indicated in the Supplementary Table S1.

model, DU145/DU145-Rx using the same dose escalation strategy. DU145-Rx cells exhibit a significantly increased IC_{50} for docetaxel (Supplementary Fig. S1A) and increased clonogenic capacity following docetaxel treatment (Supplementary Fig. S1B), when compared with their parental cells. Neither cell line model exhibited any changes in P-glycoprotein activity, consistent with docetaxel resistance not being mediated by drug efflux (Supplementary Fig. S1C; ref. 18).

To quantitatively characterize the perturbed tyrosine phosphorylation events associated with docetaxel chemoresistance, we utilized an immunoaffinity-coupled mass spectrometry (LC/MS-MS) approach in combination with SILAC (Fig. 1A) to compare docetaxel-sensitive cells (PC3 and DU145) with their docetaxel-resistant counterparts (PC3-Rx and DU145-Rx). This identified 365 tyrosine phosphorylation sites derived from 215 unique proteins exhibiting differential phosphorylation. A ranking of individual phosphosites with up- or downregulated phosphorylation according to their SILAC ratios demonstrated a large overlap of phosphorylation changes in PC3-Rx and DU145-Rx cells (Fig. 1B and Supplementary Table S1). A striking characteristic of the phosphorylation profile associated with docetaxel-resistant cell lines was the enrichment for proteins involved in regulating focal adhesions and the actin cytoskeleton, such as ACTN1/4, FAK, BCAR1, VIM, PDLIM5, CAV, PAX, and ANXA1. Mapping protein–protein interactions among the differentially phosphorylated proteins highlighted the presence of interaction "hubs" that centered on members of these pathways, such as FAK, VIM, and ACTN1 (Fig. 2A). Furthermore, pathway enrichment analysis revealed that "regulation of actin cytoskeleton" and "focal adhesion" were the top 2 pathways enriched in PC3-Rx and DU145-Rx cells (the corrected $P < 0.05$; Fig. 2B). The top 10 upregulated

Published OnlineFirst November 5, 2013; DOI: 10.1158/1535-7163.MCT-13-0225-T

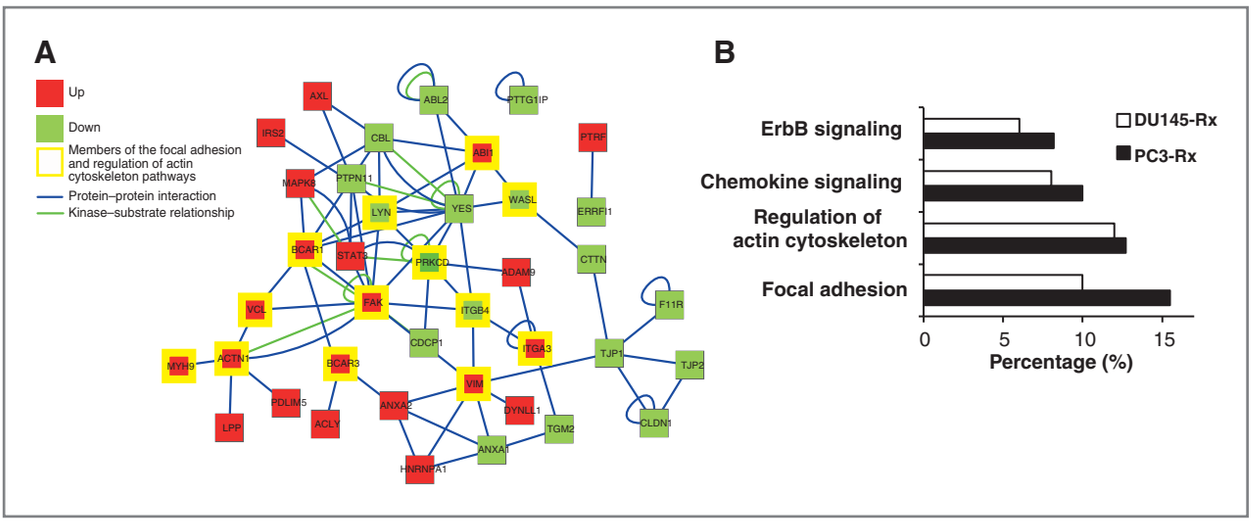

Figure 2. Characterization of tyrosine kinase signaling networks in docetaxel-resistant cell lines. A, network analysis on differentially phosphorylated proteins characteristic of DU145-Rx cells versus the DU145 parental line. Upregulated phosphorylation sites in DU145-Rx cells are indicated in red and downregulated phosphorylation sites are indicated in green. Blue edges indicate protein–protein interactions, whereas green edges indicate kinase–substrate relationships. Members of the "focal adhesion" and "regulation of actin-cytoskeleton" pathways are highlighted in yellow. B, pathway enrichment analysis was performed on phosphorylation sites differentially phosphorylated between PC3-Rx and DU145-Rx cells and their drug sensitive counterparts. The top 4 pathways enriched in both cell lines are shown (the corrected $P < 0.05$).

phosphorylation sites common to both Rx cell lines included sites from 3 kinases (FAK, AXL, HIPK3), 1 protease (ADAM9), and 3 actin cytoskeletal proteins (ACTN1, VIM, PDLIM5; Table 1). Of these, seven are potential therapeutic targets amenable to inhibition by small molecule drugs. Strikingly, the autophosphorylation and SRC binding site, Y397, and sites located at the kinase domain activation loop, Y576 and Y577, of FAK were included among the top phosphorylated sites.

FAK regulation and function in docetaxel-sensitive and -resistant prostate cancer cells

Consistent with the profiling data, immunoblotting revealed that both chemoresistant cell lines showed significantly enhanced FAK phosphorylation on Y397 and Y576 residues compared with the parental cells (Figs. 3A–C and 4A–C). Of note, total FAK expression was not significantly altered. To interrogate the role of FAK-mediated signaling in chemoresistance, we utilized PF-00562271 (27),

Table 1. Characteristics of the top 10 upregulated tyrosine phosphorylation sites found common to both docetaxel-resistant prostate cancer models, PC3/PC3-Rx and DU145/DU145-Rx

Position	Gene name	DU145-Rx SILAC Ratio	PC3-Rx SILAC Ratio	Peptide sequence	Targeted Strategy
246	ACTN1	1.68	3.51	_AIMTYVSSFY(ph)HAFSGAQK_	—
61	VIM	1.27	2.22	_SLYASSPGGVY(ph)ATR_	Withaferin-A
702	AXL;UFO	1.29	2.03	_IYNGDY(ph)YR_	R428, XL-880
359	HIPK3;DYRK6	1.38	1.95	_TVCSTY(ph)LQSR_	—
53	VIM	1.34	1.91	_SLY(ph)ASSPGGVYATR_	Withaferin-A
397	FAK	1.87	1.65	_THAVSVSETDDY(ph) AEIIDEEDTYTMPSTR_	PF-00562271, PF-04554878, Y11, Y15, GSK-2256098, TAE-226, PND-1186
577	FAK	1.79	1.51	_YMEDSTYY(ph)K_	PF-00562271, PF-04554878, GSK-2256098, TAE-226, PND-1186
576	FAK	1.76	1.42	_YMEDSTY(ph)YK_	PF-00562271, PF-04554878, GSK-2256098, TAE-226, PND-1186
815	ADAM9	1.33	1.72	_VSSQGNLIPARPAPAPPLY(ph)SSLT_	ProA9
251	PDLIM5	1.63	1.67	_YTEFY(ph)HVPTHSDASK_	—

Published OnlineFirst November 5, 2013; DOI: 10.1158/1535-7163.MCT-13-0225-T

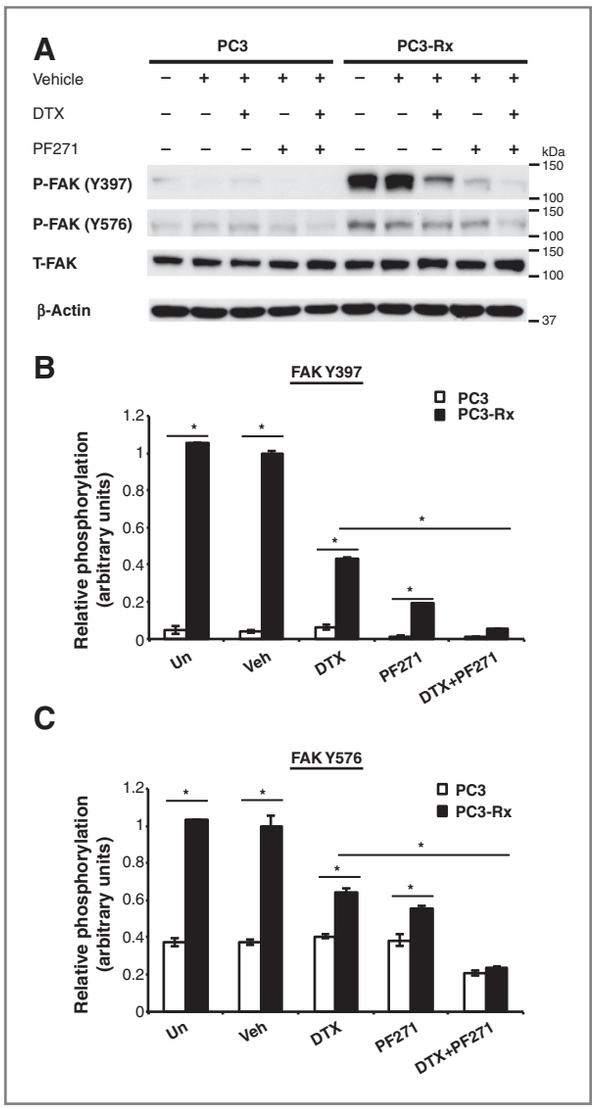

Figure 3. Regulation of FAK phosphorylation in docetaxel-sensitive and -resistant PC3 cells. A, immunoblotting analysis. PC3/PC3-Rx cells were treated with/without docetaxel (DTX; 8 ng/mL) ± PF-00562271 (PF271; 100 nmol/L) for 24 hours. Total cell lysates were immunoblotted as indicated. B and C, quantitative analysis of the immunoblots described above using ImageJ software. FAK phosphorylation at Y397 (B) and Y576 (C) was normalized for total FAK levels and is expressed relative to vehicle (saline and DMSO) controls. Results are shown as mean ± SEM for each data point in three independent experiments. *, $P < 0.0001$.

a small-molecule FAK TKI, and tested the ability of docetaxel alone or docetaxel + PF-00562271 cotreatment to kill resistant cells. In the resistant cells, treatment with PF-00562271 reduced phosphorylation on both Y397 and Y576, whereas in the sensitive cells, the effects of this TKI were more modest (Figs. 3B and C and 4B and C). Interestingly, Docetaxel administration also reduced FAK phosphorylation on both sites in the resistant cells, but combined treatment with PF-00562271 and docetaxel led to a further diminution in FAK phosphorylation, such that it returned to levels comparable with that of the parental cells.

Both the PC3-Rx and DU145-Rx cell lines showed significantly enhanced Akt phosphorylation (S473 and T308) with or without docetaxel (Supplementary Fig. S2). Strikingly, the cotreatment further inhibited Akt phosphorylation compared with docetaxel alone. However, PF-00562271 alone had no effect on Akt phosphorylation. ERK activation was not enhanced in either docetaxel-resistant cell line (data not shown).

We then determined the effect of FAK inhibition on the sensitivity of the parental and resistant cells to docetaxel. Administration of PF-00562271 alone did not affect the

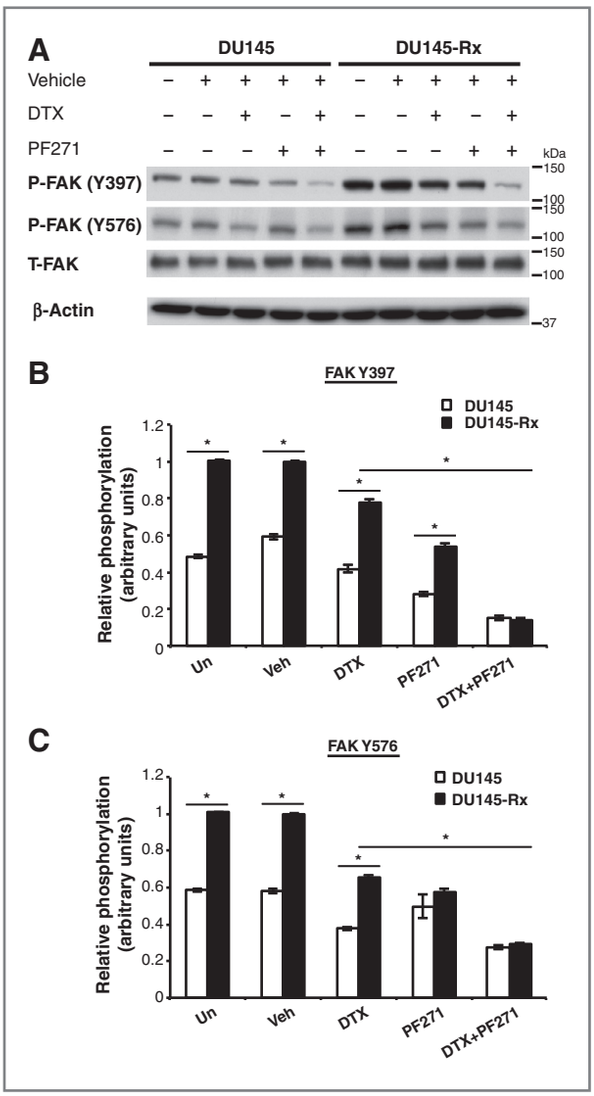

Figure 4. Regulation of FAK phosphorylation in docetaxel-sensitive and -resistant DU145 cells. A, immunoblotting analysis. DU145/DU145-Rx cells were treated with/without docetaxel (DTX; 8 ng/mL) ± PF-00562271 (PF271; 100 nmol/L) for 24 hours. Total cell lysates were immunoblotted as indicated. B and C, quantitative analysis of the immunoblots described above using ImageJ software. FAK phosphorylation at Y397 (B) and Y576 (C) was normalized for total FAK levels and is expressed relative to vehicle (saline and DMSO) controls. Results are shown as mean ± SEM for each data point in three independent experiments. *, $P < 0.0001$.

Published OnlineFirst November 5, 2013; DOI: 10.1158/1535-7163.MCT-13-0225-T

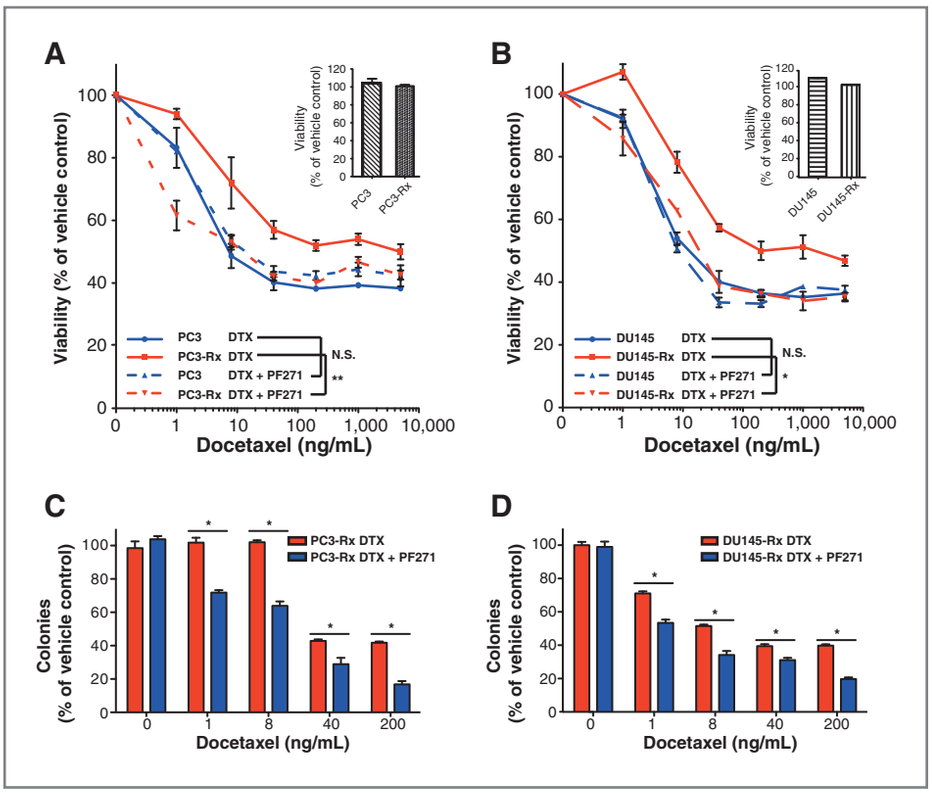

Figure 5. The FAK inhibitor PF-00562271 sensitizes chemoresistant prostate cancer cells to docetaxel. A and B, dose response curves assessing the effect of individual and combination drug treatments on cell viability. The PC3/PC3-Rx (A) and DU145/DU145-Rx (B) models were treated with increasing doses of docetaxel ± PF-00562271 (PF271; 100 nmol/L) for 24 hours. Cell viability is expressed relative to vehicle (saline and DMSO) control. Results are shown as mean ± SEM for each data point in three independent experiments with triplicate samples. *, $P < 0.0049$; **, $P < 0.0004$. Insets indicate that PF-00562271 alone has no effect on viability in PC3/PC3-Rx and DU145/DU145-Rx cells. C and D, effect of drug treatments on colony-forming ability. The PC3/PC3-Rx (C) and DU145/DU145-Rx (D) models were treated with increasing doses of docetaxel ± PF-00562271 (PF271; 100 nmol/L) for 24 hours. Colonies are expressed relative to vehicle (saline and DMSO) control. Results are shown as mean ± SEM for each data point in three independent experiments with triplicate samples. *, $P < 0.0001$.

viability of either cell type (Fig. 5A and B). Treatment with PF-00562271 did not affect the sensitivity of parental PC3 or DU145 cells to docetaxel. In contrast, it reversed the chemoresistant phenotypes of both the PC3-Rx and DU145-Rx cell lines. Cotreatment with PF-00562271/docetaxel resulted in a 35- and 28-fold IC_{50} decrease in PC3-Rx and DU145-Rx cells, respectively, when compared with docetaxel alone ($P < 0.0004$ and 0.0049, respectively; Table 2). In addition, while PF-00562271 alone did not affect colony formation, coadministration of this TKI with docetaxel significantly reduced colony formation by Rx cells compared with docetaxel alone (Fig. 5C and D). These data indicate that the elevated FAK activity in the resistant models mediates docetaxel resistance and can be targeted to resensitize the cells to the drug.

Effect of docetaxel and PF-00562271 cotreatment on apoptotic cell death

Consistent with the cell viability data, a higher percentage of parental cells underwent apoptosis upon docetaxel treatment compared with their Rx counterparts, as determined by assaying for cells in sub-G_1 phase (Fig. 6A and B)

Table 2. The IC_{50} values (docetaxel concentration required to inhibit 50% of viability) of docetaxel and cotreatment in PC3/PC3-Rx and DU145/DU145-Rx cells

	IC_{50} (ng/mL)			
	PC3	PC3-Rx	DU145	DU145-Rx
Docetaxel	28.22	698.91	26.54	1,288.41
Docetaxel + PF-00562271	32.59	19.86	18.51	45.42

Published OnlineFirst November 5, 2013; DOI: 10.1158/1535-7163.MCT-13-0225-T

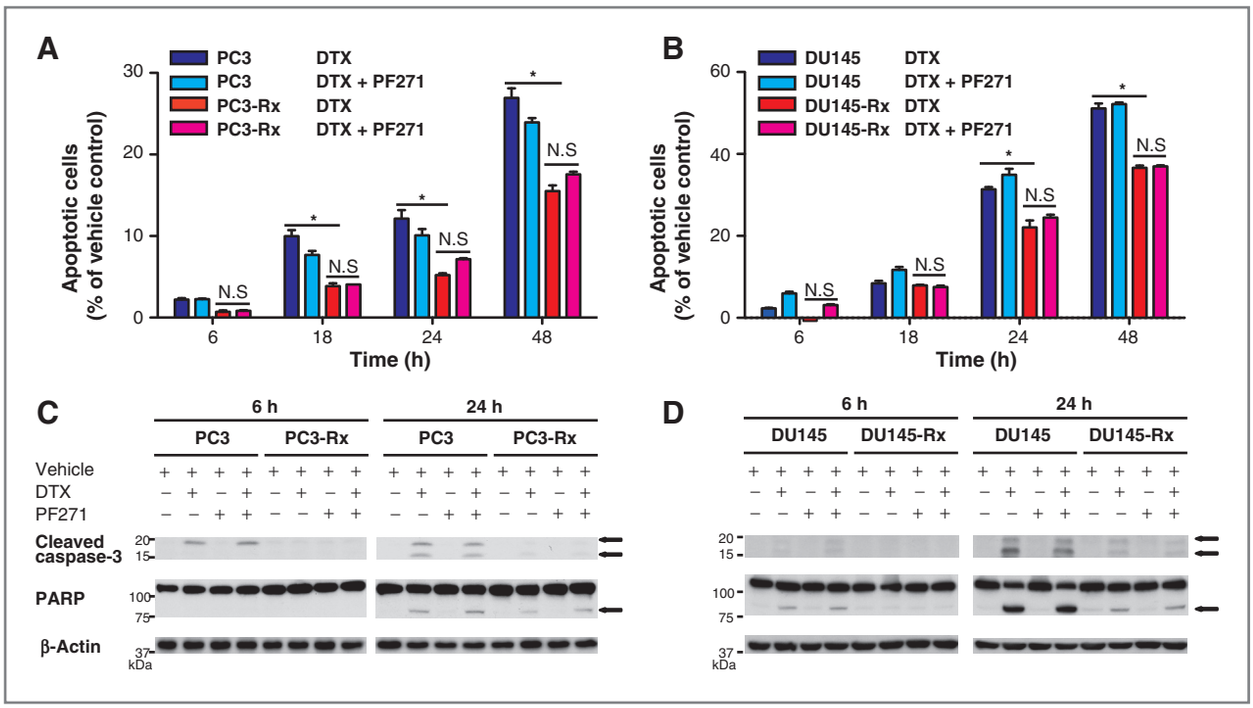

Figure 6. Docetaxel/PF-00562271–induced cell death in docetaxel-resistant prostate cancer cells is not via enhanced apoptosis. A and B, quantification of PC3/PC3-Rx (A) and DU145/DU145-Rx (B) cells undergoing apoptosis during docetaxel (DTX; 8 ng/mL) ± PF-00562271 (PF271; 100 nmol/L) treatments. Quantification of apoptosis is adjusted relative to vehicle (DMSO and saline) control. Results are shown as mean ± SEM for each data point in three independent experiments with triplicate samples. *, $P < 0.0001$. C and D, effect of individual and combination treatments on activation of apoptosis was measured by immunoblotting for the indicated apoptotic markers. Cleaved or activated forms of these markers are indicated with arrows.

and immunoblotting for cleaved caspase-3 and PARP (Fig. 6C and D). However, while cotreatment with PF-00562271 and docetaxel markedly reduced the viability of the Rx cells, it did not induce increased apoptosis compared with the administration of docetaxel alone. Furthermore, pharmacologic blockage of the apoptotic pathway using Z-VAD-FMK, a pan-caspase inhibitor, did not rescue the decreased cell viability resulting from PF-00562271/docetaxel cotreatment of PC3-Rx and DU145-Rx cells, in contrast with the effect of this inhibitor on docetaxel ± PF-00562271 treatment of parental cells (Fig. 7A and B). These data indicate that the reduction in cell viability induced by cotreatment of Rx cells is not via enhanced apoptosis.

Effect of docetaxel and PF-00562271 cotreatment on autophagic cell death

Next, we sought to determine whether type II programmed cell death, also known as autophagic cell death, was involved (28). One of the precursor signatures of autophagy is reduced phosphorylation of mTOR. Strikingly, cotreatment, but not administration of either agent alone, resulted in a marked attenuation of mTOR phosphorylation at 6 hours, but not at 24 hours (Fig. 8A). In addition, LC3B conversion and degradation of p62 are downstream features of induction of autophagy. During the autophagy process, LC3B is cleaved to generate LC3B-I, which is then converted to membrane-bound LC3B-II via lipidation. LC3B conversion can be quantified by the ratio of LC3B-II relative to LC3B-I (29, 30).

While cotreatment of PF-00562271 and docetaxel for 24 hours did not affect relative LC3B-II or p62 levels compared with docetaxel alone in the parental PC3 cells (Fig. 8A), coadministration resulted in a significant enhancement of relative LC3B-II accumulation and a marked decrease in p62 expression in PC3-Rx cells (Fig. 8A and B). However, unlike in the PC3 model, where docetaxel only induced autophagy in the resistant cells, docetaxel monotherapy induced autophagy in both DU145 and DU145-Rx cells, but the combination treatment resulted in a significant enhancement of relative LC3B-II accumulation and p62 degradation specifically in DU145-Rx cells in comparison with docetaxel alone (Fig. 8C and Supplementary Fig. S3). While administration of 3-MA, a pharmacologic inhibitor of autophagosome formation, did not affect the sensitivity of Rx cells to docetaxel alone, it significantly attenuated co-treatment–induced cell death (Fig. 9A and B). We next used siRNA to transiently knock down Atg5, a gene essential for autophagosome formation (Fig. 9C). This also rescued PC3-Rx cells from cotreatment–induced cell death, but did not affect sensitivity to docetaxel alone (Fig. 9D). These data indicate that the enhanced efficacy of cotreatment in reducing viability and overcoming the chemoresistant phenotypes in Rx cells is mediated via increased autophagy.

Published OnlineFirst November 5, 2013; DOI: 10.1158/1535-7163.MCT-13-0225-T

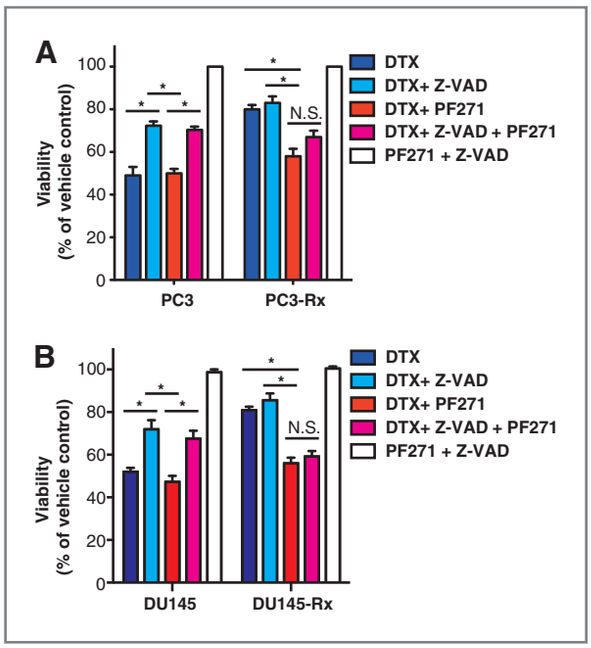

Figure 7. Docetaxel/PF-00562271–induced cell death in docetaxel-resistant cells is not rescued by inhibition of caspase-dependent apoptosis. Effect of caspase inhibition on cell viability following drug treatment. Viable PC3/PC3-Rx (A) and DU145/DU145-Rx (B) cells following 24-hour docetaxel (DTX; 8 ng/mL) ± PF-00562271 (PF271; 100 nmol/L) ± Z-VAD-FMK (100 μmol/L) treatments are expressed relative to vehicle (saline and DMSO) control. Results are shown as mean ± SEM for each data point in three independent experiments with triplicate samples. *, $P < 0.0001$.

Discussion

To date, the targeting of FAK has faced significant challenges in the clinic. Early studies in ovarian cancer cell lines and xenografts demonstrated that knockdown of FAK expression enhanced docetaxel efficacy in docetaxel-sensitive and docetaxel-resistant models *in vitro* and *in vivo* (31, 32). Subsequently, TAE226, a TKI that targets FAK and IGF-1R, was demonstrated to enhance docetaxel cytotoxicity (33); however, at this point, development stalled due to the drug failing clinical trials. Other first-generation FAK TKIs had problems with compensatory upregulation of the FAK homolog, Pyk2, which affected clinical efficacy (34). Newer FAK TKIs targeting FAK and Pyk2, PF-00562271, and its second-generation PF-04554878, were well tolerated in phase I clinical trials (35, 36), and the latter is currently in phase Ib and II clinical trials (37). While the efficacy of combining PF-00562271 with cytotoxic agents has not been reported, coadministration of this TKI with sunitinib in a hepatocellular carcinoma xenograft model exhibited a significantly greater effect than monotherapy, blocking tumor growth and tumor recovery after treatment (38). PF-00562271 is a potent inhibitor of CYP3A, whereas PF-04554878 is a weak CYP3A inhibitor with a low potential for CYP3A drug–drug interaction (35, 36), making this second-generation compound the preferred FAK inhibitor for development in combination with cytotoxics. Our preclinical data support the establishment of clinical trials testing docetaxel in combination with PF-04554878 in men with metastatic CRPC.

Interrogation of the functional role of FAK in the chemoresistant cells revealed that while treatment with PF-00562271 significantly decreased FAK phosphorylation, this did not affect cell viability *in vitro*, consistent with other studies using small-molecule FAK inhibitors and cells grown under monolayer conditions (19). Instead, a significant reduction in cell viability was only observed in the presence of docetaxel, where coadministration of a FAK inhibitor resensitized the cells to docetaxel chemotherapy. This reflects a novel effect of docetaxel, where treatment with this drug reduced FAK phosphorylation on both Y397 and Y576, and coadministration with FAK inhibitor resulted in an additive diminution of FAK phosphorylation back to the levels characteristic of parental cells. The activity of docetaxel on focal adhesion signaling likely reflects its activity as a microtubule-targeting agent, as microtubules interact with focal adhesions and regulate their turnover (39). Support for this model is provided by studies on a different microtubule-targeting agent, laulimalide, which also decreases FAK phosphorylation (40). Of note, while FAK couples to PI3-kinase/Akt signaling via recruitment of the p85 subunit of PI3-kinase to phosphorylated Y397 (41), individual treatment with either docetaxel or a FAK inhibitor was insufficient to significantly downregulate Akt/mTOR signaling *in vitro*. Instead, this was only achieved by the combination treatment. Because mTOR negatively regulates autophagy, we propose that the combination therapy reduces mTOR activation below a certain threshold and triggers an autophagic response and ultimately cytotoxicity. Whether the effect of the combination treatment on Akt and mTOR is entirely due to a reduction in FAK activation requires further clarification.

While docetaxel induced apoptotic cell death in the parental cells, chemosensitization conferred by the combination treatment was not associated with increased apoptosis in the drug-resistant cells. This is in contrast with previous studies involving targeting of FAK in combination with administration of chemotherapeutic agents. For example, Halder and colleagues (33) reported increased tumor cell apoptosis in ovarian cancer cell line xenografts when these were subjected to TAE-226/docetaxel coadministration, compared with either treatment alone. In addition, Golubovskaya and colleagues (42) detected enhanced apoptotic cell death when Y15, a small-molecule agent that targets the FAK autophosphorylation site, was administered to glioblastoma cell lines in combination with temozolomide. Consequently, the ability of FAK-directed agents to induce apoptosis appears to be dependent on context and the targeting strategy employed.

Interestingly, in our study, coadministration of PF-00562271 and docetaxel was also not associated with enhanced caspase-independent cell death, as indicated

Published OnlineFirst November 5, 2013; DOI: 10.1158/1535-7163.MCT-13-0225-T

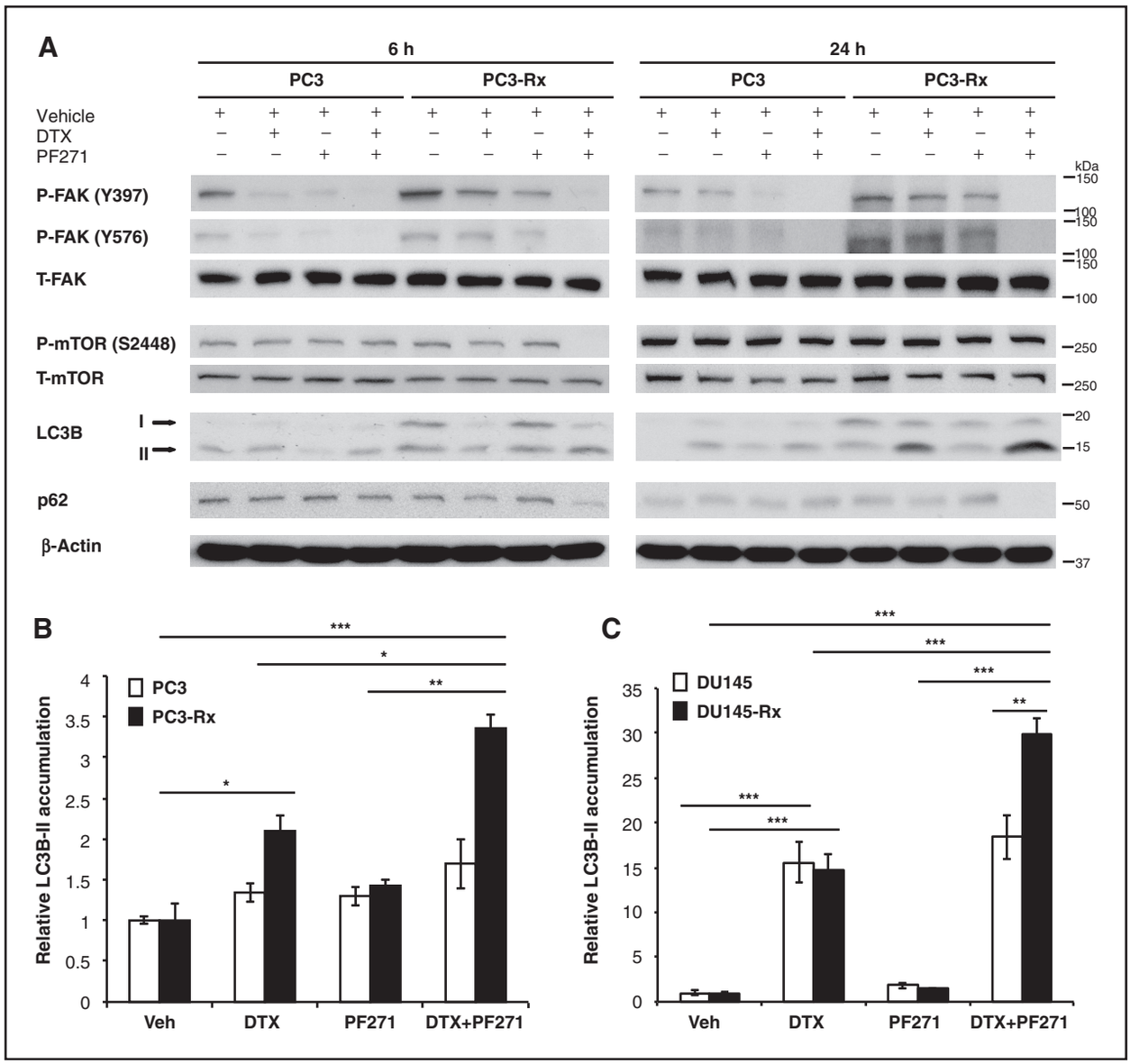

Figure 8. Cotreatment-induced cell death in docetaxel-resistant cells is associated with enhanced autophagy. A, the effect of individual and combination treatments on the induction of autophagy. Cells were treated with docetaxel (DTX; 8 ng/mL) ± PF-00562271 (PF271; 100 nmol/L) for 6 and 24 hours. Total cell lysates were immunoblotted as indicated. B and C, quantification of relative LC3B-II levels of PC3/PC3-Rx (B) and DU145/DU145-Rx (C) cells. LC3B-II expression was normalized for LC3B-I and loading (β-actin) controls, and is expressed relative to vehicle (saline and DMSO). Results are shown as mean ± SEM for each data point in three independent experiments with triplicate samples. Asterisks indicate the following *P* value ranges: *, $P < 0.05$; **, $P < 0.001$; and ***, $P < 0.0001$.

by increased mitochondrial outer membrane permeability (data not shown). Instead, cotreatment with FAK inhibitor and docetaxel resulted in increased autophagy, and a causative role for this process in the enhanced cytotoxicity induced by the cotreatment was confirmed by pharmacologic and genetic approaches. These data are of interest in light of a previous study where knockdown of p130Cas, which signals downstream of FAK, resulted in enhanced autophagy in ovarian cancer cells (43) and add further weight to the emerging concept that the role of autophagy in cancer development and progression is highly context dependent. Thus, while specific autophagy genes, such as Beclin-1, can act as tumor suppressors (44), and particular drug regimens can exert cytotoxicity through autophagic cell death (45, 46) induction of autophagy can also confer drug resistance to cancer cells, for example, against the TKIs erlotinib (47) and saracatinib (48). Moreover, our work also emphasizes how FAK signaling can exert contrasting effects on autophagy and cell survival. Recent work from Sandilands and colleagues using a skin

Published OnlineFirst November 5, 2013; DOI: 10.1158/1535-7163.MCT-13-0225-T

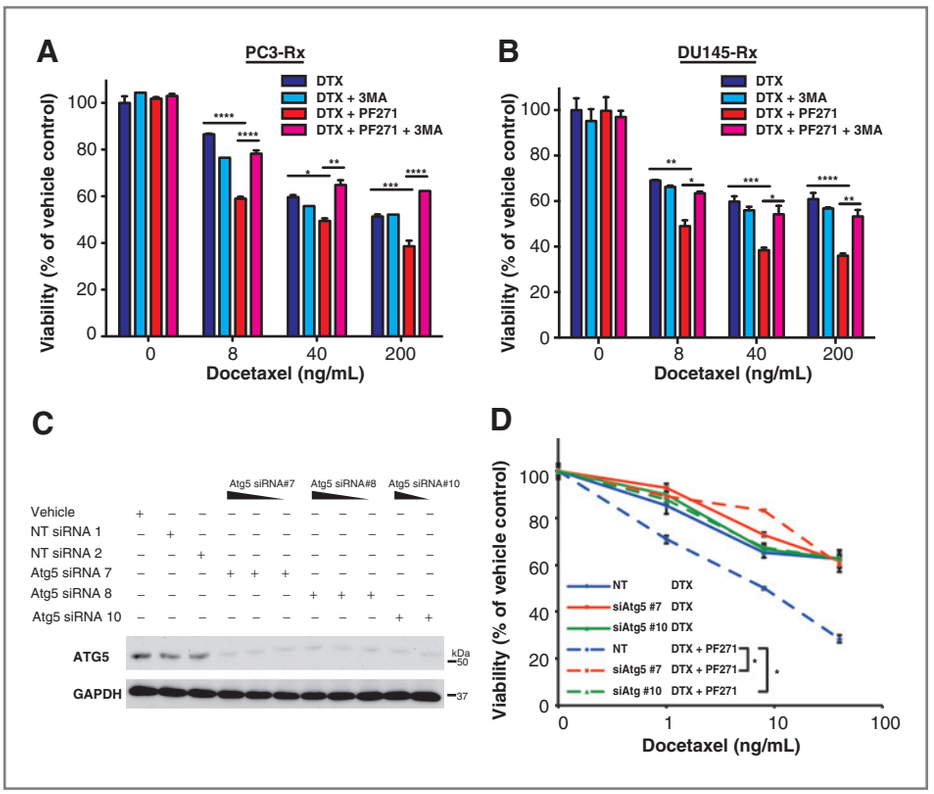

Figure 9. Cotreatment-induced cell death in docetaxel-resistant cells is rescued by inhibition of autophagy. A and B, effect of a pharmacologic inhibitor of autophagosome formation on docetaxel and drug combination-induced cell death in docetaxel-resistant cells. Viable PC3-Rx (A) and DU145-Rx (B) cells following 24 hour docetaxel (as indicated) ± PF-00562271 (PF271; 100 nmol/L) ± 3-methyladenine (3-MA; 5 mmol/L) treatments were expressed relative to vehicle (saline and DMSO) control. Results are shown as mean ± SEM for each data point in three independent experiments with triplicate samples. Asterisks indicate the following *P* value ranges: *, $P < 0.05$; **, $P < 0.01$; ***, $P < 0.001$; ****, $P < 0.0001$. C, confirmation of siRNA-mediated Atg5 knockdown. Cells were transiently transfected with non-targeting or Atg5 siRNAs for 48 hours. Total lysates were immunoblotted for Atg5 and GAPDH (loading control). D, effect of Atg5 knockdown on viability of docetaxel and drug combination-treated cells. PC3-Rx cells were transiently transfected with either nontargeting or Atg5 siRNA #7 or 10 for 48 hours, then were treated with docetaxel (as indicated) ± PF-00562271 (PF271; 100 nmol/L) for 24 hours. Viable cells were expressed relative to vehicle (saline and DMSO) control. Results are shown as mean ± SEM for each data point in three independent experiments with triplicate samples. *, $P < 0.05$.

cancer model demonstrated that components of the autophagy pathway are intimately associated with focal adhesions, and that loss of FAK can trigger an apoptotic response, unless the active Src released upon FAK ablation is subject to autophagic targeting (49). This led to the suggestion that combining FAK and/or Src inhibitors with an autophagy inhibitor may reduce the viability of cancer cells. Since, in our study, blocking autophagy rescued prostate cancer cells from a combination treatment involving FAK inhibition, this highlights how such strategies should be applied in a selective manner.

While PF-00562271 and PF-04554878 monotherapies were well tolerated in phase I trials (35, 36), a clear clinical application for FAK TKIs has yet to be identified. According to the molecularly characterized preclinical data presented in this study, we have identified a potential clinical niche for selective FAK TKIs, where coadministration with docetaxel may be used in patients with CRPC to overcome chemoresistance, providing the basis for further clinical development.

Disclosure of Potential Conflicts of Interest

S.M. Shreeve has stock ownership interest in Pfizer Oncology. L.G. Horvath has an honorarium for being on the organising committee of the Australian Pfizer Oncology Forum and attended a research forum with Pfizer in La Jolla, California, paid for by Pfizer. No potential conflicts of interest were disclosed by the other authors.

Authors' Contributions

Conception and design: B.Y. Lee, S.M. Shreeve, L.G. Horvath, R.J. Daly
Development of methodology: B.Y. Lee, S.M. Shreeve, L.G. Horvath, R.J. Daly
Acquisition of data (provided animals, acquired and managed patients, provided facilities, etc.): B.Y. Lee, F. Hochgräfe, H.-M. Lin, L. Castillo, M.J. Raftery
Analysis and interpretation of data (e.g., statistical analysis, biostatistics, computational analysis): B.Y. Lee, F. Hochgräfe, J. Wu, L.G. Horvath, R.J. Daly
Writing, review, and/or revision of the manuscript: B.Y. Lee, S.M. Shreeve, L.G. Horvath, R.J. Daly
Administrative, technical, or material support (i.e., reporting or organizing data, constructing databases): B.Y. Lee, L. Castillo
Study supervision: L.G. Horvath, R.J. Daly

Acknowledgments

The authors gratefully acknowledge the late Professor Rob Sutherland for his intellectual input into this paper.

Grant Support

This work was supported by a Program Grant (535903) from the National Health and Medical Research Council of Australia (to R.J. Daly, E.A. Musgrove, R.L. Sutherland, C.J. Ormandy, J.G. Kench, A.V. Biankin, E.K. Millar, L.G. Horvath, S.A. O'Toole), a Program Grant (10/TPG/1-04) from the Cancer Institute NSW (to L.G. Horvath), and by Cancer Australia/Prostate Cancer Foundation of Australia (596858; to L.G. Horvath, M. Boyer, R.J. Daly, R.L. Sutherland). B.Y. Lee is the recipient of a Research Scholar Award (09/RSA/1-20) from the Cancer Institute of New South Wales and an Australian Postgraduate Award from the University of New South Wales.

Received May 1, 2013; revised October 25, 2013; accepted October 29, 2013; published OnlineFirst November 5, 2013.

References

1. Jemal A, Bray F, Center MM, Ferlay J, Ward E, Forman D. Global cancer statistics. CA Cancer J Clin 2011;61:69–90.
2. Tannock IF, de Wit R, Berry WR, Horti J, Pluzanska A, Chi KN, et al. Docetaxel plus prednisone or mitoxantrone plus prednisone for advanced prostate cancer. N Engl J Med 2004;351:1502–12.
3. Petrylak DP, Tangen CM, Hussain MH, Lara PNJr, Jones JA, Taplin ME, et al. Docetaxel and estramustine compared with mitoxantrone and prednisone for advanced refractory prostate cancer. N Engl J Med 2004;351:1513–20.
4. Sanchez C MP, Contreras HR, Vergara J, McCubrey JA, Huidobro C, Castellon EA. Expression of multidrug resistance proteins in prostate cancer is related with cell sensitivity to chemotherapeutic drugs. Prostate 2009;69:1448–59.
5. Sowery RD, Hadaschik BA, So AI, Zoubeidi A, Fazli L, Hurtado-Coll A, et al. Clusterin knockdown using the antisense oligonucleotide OGX-011 re-sensitizes docetaxel-refractory prostate cancer PC-3 cells to chemotherapy. BJU Int 2008;102:389–97.
6. Murphy L, Henry M, Meleady P, Clynes M, Keenan J. Proteomic investigation of taxol and taxotere resistance and invasiveness in a squamous lung carcinoma cell line. Biochim Biophys Acta 2008; 1784:1184–91.
7. Sapi E, Alvero AB, Chen W, O'Malley D, Hao XY, Dwipoyono B, et al. Resistance of ovarian carcinoma cells to docetaxel is XIAP dependent and reversible by phenoxodiol. Oncol Res 2004;14:567–78.
8. Haldar S, Chintapalli J, Croce CM. Taxol induces bcl-2 phosphorylation and death of prostate cancer cells. Cancer Res 1996;56:1253–5.
9. Zhong B, Sallman DA, Gilvary DL, Pernazza D, Sahakian E, Fritz D, et al. Induction of clusterin by AKT–role in cytoprotection against docetaxel in prostate tumor cells. Mol Cancer Ther 2010;9:1831–41.
10. Mathew P, Thall PF, Wen S, Bucana C, Jones D, Horne E, et al. Dynamic change in phosphorylated platelet-derived growth factor receptor in peripheral blood leukocytes following docetaxel therapy predicts progression-free and overall survival in prostate cancer. Br J Cancer 2008;99:1426–32.
11. Chi KN, Hotte SJ, Yu EY, Tu D, Eigl BJ, Tannock I, et al. Randomized phase II study of docetaxel and prednisone with or without OGX-011 in patients with metastatic castration-resistant prostate cancer. J Clin Oncol 2010;28:4247–54.
12. Mathew P, Thall PF, Bucana CD, Oh WK, Morris MJ, Jones DM, et al. Platelet-derived growth factor receptor inhibition and chemotherapy for castration-resistant prostate cancer with bone metastases. Clin Cancer Res 2007;13:5816–24.
13. Oh WK, Galsky MD, Stadler WM, Srinivas S, Chu F, Bubley G, et al. Multicenter phase II trial of the heat shock protein 90 inhibitor, retaspimycin hydrochloride (IPI-504), in patients with castration-resistant prostate cancer. Urology. 2011;78:626–30.
14. Sonpavde G, Matveev V, Burke JM, Caton JR, Fleming MT, Hutson TE, et al. Randomized phase II trial of docetaxel plus prednisone in combination with placebo or AT-101, an oral small molecule Bcl-2 family antagonist, as first-line therapy for metastatic castration-resistant prostate cancer. Ann Onco. 2012;23:1803–8.
15. Rago RP, Einstein AJr, Lush R, Beer TM, Ko YJ, Henner WD, et al. Safety and efficacy of the MDR inhibitor Incel (biricodar, VX-710) in combination with mitoxantrone and prednisone in hormone-refractory prostate cancer. Cancer Chemother Pharmacol 2003;51:297–305.
16. Saad F, Hotte S, North S, Eigl B, Chi K, Czaykowski P, et al. Randomized phase II trial of Custirsen (OGX-011) in combination with docetaxel or mitoxantrone as second-line therapy in patients with metastatic castrate-resistant prostate cancer progressing after first-line docetaxel: CUOG trial P-06c. Clin Cancer Res 2011;17:5765–73.
17. de Bono JS, Oudard S, Ozguroglu M, Hansen S, Machiels JP, Kocak I, et al. Prednisone plus cabazitaxel or mitoxantrone for metastatic castration-resistant prostate cancer progressing after docetaxel treatment: a randomised open-label trial-. Lancet. 2010;376:1147–54.
18. Zhao L, Lee BY, Brown DA, Molloy MP, Marx GM, Pavlakis N, et al. Identification of candidate biomarkers of therapeutic response to docetaxel by proteomic profiling. Cancer Res. 2009;69:7696–703
19. Hochgrafe F, Zhang L, O'Toole SA, Browne BC, Pinese M, Porta Cubas A, et al. Tyrosine phosphorylation profiling reveals the signaling network characteristics of Basal breast cancer cells. Cancer Res 2010; 70:9391–401.
20. Croucher DR, Hochgrafe F, Zhang L, Liu L, Lyons RJ, Rickwood D, et al. Involvement of Lyn and the atypical kinase SgK269/PEAK1 in a basal breast cancer signaling pathway. Cancer Res 2013;73:1969–80.
21. Xie C, Mao X, Huang J, Ding Y, Wu J, Dong S, et al. KOBAS 2.0: a web server for annotation and identification of enriched pathways and diseases. Nucleic Acids Res 2011;39:W316–22.
22. Benjamini Y, Hochberg Y. Controlling the false discovery rate - a practical and powerful approach to multiple testing. Journal of the Royal Statistical Society Series B-Methodological 1995;57:289–300.
23. Cowley MJ, Pinese M, Kassahn KS, Waddell N, Pearson JV, Grimmond SM, et al. PINA v2.0: mining interactome modules. Nucleic Acids Res 2012;40:D862–5.
24. Hornbeck PV, Kornhauser JM, Tkachev S, Zhang B, Skrzypek E, Murray B, et al. PhosphoSitePlus: a comprehensive resource for investigating the structure and function of experimentally determined post-translational modifications in man and mouse. Nucleic Acids Res 2012;40:D261–70.
25. Smoot ME, Ono K, Ruscheinski J, Wang PL, Ideker T. Cytoscape 2.8: new features for data integration and network visualization. Bioinformatics 2011;27:431–2.
26. Brummer T, Larance M, Herrera Abreu MT, Lyons RJ, Timpson P, Emmerich CH, et al. Phosphorylation-dependent binding of 14-3-3 terminates signalling by the Gab2 docking protein. EMBO J 2008; 27:2305–16.
27. Roberts WG, Ung E, Whalen P, Cooper B, Hulford C, Autry C, et al. Antitumor activity and pharmacology of a selective focal adhesion kinase inhibitor, PF-562,271. Cancer Res 2008;68:1935–44.
28. Galluzzi L, Vitale I, Abrams JM, Alnemri ES, Baehrecke EH, Blagosklonny MV, et al. Molecular definitions of cell death subroutines: recommendations of the nomenclature committee on cell death 2012. Cell Death Differ 2012;19:107–20.
29. Khan MJ, Rizwan Alam M, Waldeck-Weiermair M, Karsten F, Groschner L, Riederer M, et al. Inhibition of autophagy rescues palmitic acid-induced necroptosis of endothelial cells. J Biol Chem 2012;287: 21110–20.
30. Rodriguez-Vargas JM, Ruiz-Magana MJ, Ruiz-Ruiz C, Majuelos-Melguizo J, Peralta-Leal A, Rodriguez MI, et al. ROS-induced DNA damage and PARP-1 are required for optimal induction of starvation-induced autophagy. Cell Res 2012;22:1181–98.
31. Halder J, Landen CNJr., Lutgendorf SK, Li Y, Jennings NB, Fan D, et al. Focal adhesion kinase silencing augments docetaxel-mediated apoptosis in ovarian cancer cells. Clin Cancer Res 2005;11:8829–36.
32. Halder J, Kamat AA, Landen CNJr., Han LY, Lutgendorf SK, Lin YG, et al. Focal adhesion kinase targeting using in vivo short interfering RNA delivery in neutral liposomes for ovarian carcinoma therapy. Clin Cancer Res 2006;12:4916–24.
33. Halder J, Lin YG, Merritt WM, Spannuth WA, Nick AM, Honda T, et al. Therapeutic efficacy of a novel focal adhesion kinase inhibitor TAE226 in ovarian carcinoma. Cancer Res 2007;67:10976–83.

Published OnlineFirst November 5, 2013; DOI: 10.1158/1535-7163.MCT-13-0225-T

34. Schultze A, Fiedler W. Therapeutic potential and limitations of new FAK inhibitors in the treatment of cancer. Expert Opin Investig Drugs 2010; 19:777–88.
35. Infante JR, Camidge DR, Mileshkin LR, Chen EX, Hicks RJ, Rischin D, et al. Safety, pharmacokinetic, and pharmacodynamic phase I dose-escalation trial of PF-00562271, an inhibitor of focal adhesion kinase, in advanced solid tumors. J Clin Oncol 2012;30:1527–33.
36. Jones SF SG, Bendell JC, Chen EX, Bedard P, Cleary JM, Pandya S, et al. Phase I study of PF-04554878, a second-generation focal adhesion kinase (FAK) inhibitor, in patients with advanced solid tumors. J Clin Oncol 29: 2011 (suppl; abstr 3002).
37. ClinicalTrials.gov; 2013. Available from: http://clinicaltrials.gov/
38. Bagi CM, Christensen J, Cohen DP, Roberts WG, Wilkie D, Swanson T, et al. Sunitinib and PF-562,271 (FAK/Pyk2 inhibitor) effectively block growth and recovery of human hepatocellular carcinoma in a rat xenograft model. Cancer Biol Ther 2009;8:856–65.
39. Stehbens S, Wittmann T. Targeting and transport: how microtubules control focal adhesion dynamics. J Cell Biol 2012;198:481–9.
40. Lu H, Murtagh J, Schwartz EL. The microtubule binding drug laulimalide inhibits vascular endothelial growth factor-induced human endothelial cell migration and is synergistic when combined with docetaxel (taxotere). Mol Pharmacol 2006;69:1207–15.
41. Akagi T, Murata K, Shishido T, Hanafusa H. v-Crk activates the phosphoinositide 3-kinase/AKT pathway by utilizing focal adhesion kinase and H-Ras. Mol Cell Biol 2002;22:7015–23.
42. Golubovskaya VM, Huang G, Ho B, Yemma M, Morrison CD, Lee J, et al. Pharmacologic blockade of FAK autophosphorylation decreases human glioblastoma tumor growth and synergizes with temozolomide. Mol Cancer Ther 2013;12:162–72.
43. Nick AM, Stone RL, Armaiz-Pena G, Ozpolat B, Tekedereli I, Graybill WS, et al. Silencing of p130cas in ovarian carcinoma: a novel mechanism for tumor cell death. J Natl Cancer Inst 2011;103: 1596–612.
44. Liang XH, Jackson S, Seaman M, Brown K, Kempkes B, Hibshoosh H, et al. Induction of autophagy and inhibition of tumorigenesis by beclin 1. Nature 1999;402:672–6.
45. Ling YH, Aracil M, Zou Y, Yuan Z, Lu B, Jimeno J, et al. PM02734 (elisidepsin) induces caspase-independent cell death associated with features of autophagy, inhibition of the Akt/mTOR signaling pathway, and activation of death-associated protein kinase. Clin Cancer Res 2011;17:5353–66.
46. Chang KY, Tsai SY, Wu CM, Yen CJ, Chuang BF, Chang JY. Novel phosphoinositide 3-kinase/mTOR dual inhibitor, NVP-BGT226, displays potent growth-inhibitory activity against human head and neck cancer cells in vitro and in vivo. Clin Cancer Res 2011;17:7116–26.
47. Lee JG, Wu R. Combination erlotinib-Cisplatin and atg3-mediated autophagy in erlotinib resistant lung cancer. PLoS ONE. 2012;7: e48532.
48. Wu Z, Chang PC, Yang JC, Chu CY, Wang LY, Chen NT, et al. Autophagy blockade sensitizes prostate cancer cells towards Src family kinase inhibitors. Genes Cancer 2010;1:40–9.
49. Sandilands E, Serrels B, McEwan DG, Morton JP, Macagno JP, McLeod K, et al. Autophagic targeting of Src promotes cancer cell survival following reduced FAK signalling. Nat Cell Biol 2012;14:51–60.